Carriage of three plasmids in a single human clinical isolate of Clostridioides difficile

Roseboom, A.M.; Ducarmon, Q.R.; Hornung, B.V.H.; Harmanus, C.; Crobach, M.J.T.; Kuijper, E.J.; ... ; Smits, W.K.

Plasmid 125 (2023) 102669

Contents lists available at ScienceDirect

Plasmid

journal homepage: www.elsevier.com/locate/yplas

Short Communication

Carriage of three plasmids in a single human clinical isolate of *Clostridioides difficile*

Anna M. Roseboom [a], Quinten R. Ducarmon [a], Bastian V.H. Hornung [a], Céline Harmanus [a], Monique J.T. Crobach [a], Ed J. Kuijper [a], Rolf H.A.M. Vossen [b], Susan L. Kloet [b], Wiep Klaas Smits [a,c,*]

[a] Department of Medical Microbiology and Leiden University Center of Infectious Diseases (LU-CID), Leiden University Medical Center, Leiden, the Netherlands
[b] Department of Human Genetics, Leiden Genome Technology Center, Leiden University Medical Center, Leiden, the Netherlands
[c] Centre for Microbial Cell Biology, Leiden, the Netherlands

ARTICLE INFO

Keywords:
Complete genome sequence
Plasmid compatibility
C. difficile
Plasmid carriage
Extrachromosomal DNA
C. difficile plasmids

ABSTRACT

A subset of clinical isolates of *Clostridioides difficile* contains one or more plasmids and these plasmids can harbor virulence and antimicrobial resistance determinants. Despite their potential importance, *C. difficile* plasmids remain poorly characterized. Here, we provide the complete genome sequence of a human clinical isolate that carries three high-copy number plasmids from three different plasmid families that are therefore compatible. For two of these, we identify a region capable of sustaining plasmid replication in *C. difficile* that is also compatible with the plasmid pCD630 that is found in many laboratory strains. Together, our data advance our understanding of *C. difficile* plasmid biology.

1. Introduction

The Gram-positive anaerobic spore-forming bacterium *Clostridioides difficile* is responsible for healthcare-associated and community-acquired infectious diarrhea with potentially fatal consequences (Smits et al., 2016). The symptoms of a *C. difficile* infection (CDI) are related to the expression of one or more toxins, but virulence of this bacterium is multifactorial (Vedantam et al., 2012). Up to 25% of patients experiences a recurrent infection (rCDI), and this percentage can increase up to 65% if a patient has experienced one or more recurrences (Smits et al., 2016).

In many Gram-positive pathogens, virulence factors are encoded on plasmids (Adams et al., 2014; Schwarz et al., 2014). For *C. difficile*, sporadic reports indicate that toxins and resistance determinants can be carried on extrachromosomal elements (Boekhoud et al., 2020; Pu et al., 2021; Ramirez-Vargas and Rodriguez, 2020). It is estimated that ~10–70% of *C. difficile* isolates carry one or more plasmids, but information on plasmid functions is sparse (Smits et al., 2022). Though mobilization of certain *C. difficile* plasmids has been suggested (Boekhoud et al., 2020; Pu et al., 2021; Ramirez-Vargas and Rodriguez, 2020), this has not been experimentally demonstrated like for *Clostridium perfringens* plasmids (Adams et al., 2014). Based on average nucleotide identity, plasmids in sequenced *C. difficile* isolates can be grouped into at least 7 families (Hornung et al., 2019). Most plasmids belong to the pCD630/pCD-WTSI1 and pCD-ECE6/pCD6 families, but no phenotypic consequence of carrying these plasmids has been demonstrated (Hornung et al., 2019; Purdy et al., 2002; Smits et al., 2018). Plasmids from the families of pCD-ECE1 and pCD-ECE4 families range in size from 6 to 7.3 kb and 5–22 kb, respectively, and have no characterized functions (Hornung et al., 2019).

Very few replicons have been identified and almost no experimental evidence on plasmid compatibility is available. Regions sufficient for replication in *C. difficile* have been cloned from the plasmids pCD6 and pCD-METRO from strains CD6 and IB136, respectively (Boekhoud et al., 2020; Purdy et al., 2002). The pCD6 replicon encodes a RepA replication initiation protein with similarity to RepA of *C. perfringens* plasmid pIP404 (Purdy et al., 2002) and sustains a copy number of 4–10 (Ransom et al., 2015). The pCD-METRO replicon includes ORF5, a predicted

* Corresponding author at: Department of Medical Microbiology, Postzone E4-P, Leiden University Medical Center, Albinusdreef 2, Leiden 2333ZA, the Netherlands.
E-mail addresses: j.m.roseboom@biology.leidenuniv.nl (A.M. Roseboom), q.r.ducarmon@lumc.nl (Q.R. Ducarmon), c.harmanus@lumc.nl (C. Harmanus), m.j.t.crobach@lumc.nl (M.J.T. Crobach), e.j.kuijper@lumc.nl (E.J. Kuijper), r.h.a.m.vossen@lumc.nl (R.H.A.M. Vossen), s.l.kloet@lumc.nl (S.L. Kloet), w.k.smits@lumc.nl (W.K. Smits).

https://doi.org/10.1016/j.plasmid.2022.102669
Received 10 July 2022; Received in revised form 17 November 2022; Accepted 20 December 2022
Available online 23 December 2022

replication protein, and sustains a copy number > 25 (Boekhoud et al., 2020).

An *in silico* analysis of publicly available sequence data indicates that multiple plasmids can occur in a single isolate and suggests that specific families of plasmids may co-exist (Smits et al., 2022; Hornung et al., 2019), but these predictions have not been validated experimentally.

Here, we show carriage of plasmids from three different plasmid families in a single isolate of *C. difficile* derived from a human patient and report on the identification of a region sufficient for plasmid maintenance for two of these plasmids. Together, these data advance our understanding of *C. difficile* plasmid biology.

2. Materials and methods

2.1. Bacterial strain and growth conditions

All bacterial strains are listed in Table 1.

Isolates were routinely cultured on TSS plates (Tryptic Soy Agar with 5% sheep blood, bioMérieux, The Netherlands) or CLO plates (selective *C. difficile* medium containing cefoxitin, amphotericin B and cycloserine, bioMérieux, The Netherlands). Capillary electrophoresis PCR ribotyping was performed at the Dutch National Reference Laboratory for *C. difficile,* according to standard procedures (Fawley et al., 2015) and further characterized using a multiplex PCR targeting the 16S rRNA gene, *gluD*, and the genes encoding the large clostrididal toxins (*tcdA* and *tcdB*) and binary toxin (*cdtA* and *cdtB*) (ECDC, 2018).

Laboratory strains of *C. difficile* were cultured anaerobically at 37 °C in liquid BHIY (1.5% *w/v* Brain Heart Infusion [Oxoid], 0.5% w/v yeast extract [Sigma]) or on BHIY agar plates (BHIY, 1.5% agar *w/v*), supplemented with *C. difficile* selective Supplement (CDSS [Oxoid]) or colistin (50 μg/mL) and 15–25 μg/mL thiamphenicol when appropriate, in a Don Whitley VA-1000 workstation (10% CO_2, 10% H_2 and 80% N_2 atmosphere). *E. coli* strains were cultivated aerobically at 37 °C, 200 rpm in Luria-Bertani (LB) broth or on LB agar plates, supplemented with 50 μg/mL ampicillin, 25 μg/mL chloramphenicol and/or 50 μg/mL kanamycin when required. Stocks were made in 15% w/v glycerol and stored at −80 °C.

Table 1
Strains.

Strain	Description	Reference
Clostridioides difficile		
JMR1	Human clinical isolate; RT081. Contains three plasmids.	This study
JMR2	Human clinical isolate; RT081. Contains three plasmids.	This study
JMR5	Human clinical isolate; RT081. Contains pJMR5–1, pJMR5–4 and pJMR5-W plasmids.	This study
JMR7	Human clinical isolate; RT081. Contains three plasmids.	This study
630Δ*erm*	Laboratory strain; RT012.	(van Eijk et al., 2015; Hussain, 2005)
JIR8094	Laboratory strain; RT012.	(O'Connor et al., 2006)
DSMZ 28645	Laboratory strain; RT012.	(Riedel et al., 2015)
Escherichia coli		
AP24	DH5α x pAP24 (pRPF185-derived vector containing $sluc^{opt}$ and pCD6 replicon, *catP*)	(Oliveira Paiva et al., 2016)
DH5α	*fhuA2 lac(del)U169 phoA glnV44 Φ80' lacZ (del)M15 gyrA96 recA1 relA1 endA1 thi-1 hsdR17*	Laboratory stock
IB80	DH5α x pIB80 (pRPF185-derived vector containing $sluc^{opt}$ and pCD-METRO replicon, *catP*)	(Boekhoud et al., 2020)
JMR20	DH5α x pJMR20 (pAP24-derived vector containing pJMR5–1 ORF8 and flanking intergenic regions)	This study
JMR25	DH5α x pJMR25 (pAP24-derived vector containing pJMR5–1 ORF7-ORF10 and flanking intergenic regions)	This study
JMR28	DH5α x pJMR28 (pAP24-derived vector containing pJMR5-W ORF1 and flanking intergenic regions)	This study
JMR33	DH5α x pJMR33 (pAP24-derived vector containing pJMR5–4 ORF5 and flanking intergenic regions)	This study
JMR46	DH5α x pJMR46 (pAP24-derived vector containing pJMR5–4 ORF1–5 and flanking intergenic regions)	This study
JMR51	DH5α x pJMR51 (pAP24-derived vector containing pJMR5–1 ORF8–10 and flanking intergenic regions)	This study
JMR52	DH5α x pJMR52 (pAP24-derived vector containing pJMR5–1 ORF7–8 and flanking intergenic regions)	This study
JMR57	DH5α x pJMR57 (pAP24-derived vector containing pJMR5-W ORF1–4 and flanking intergenic regions)	This study

2.2. DNA isolation and whole genome sequencing of C. difficile

Initial analysis of the draft genome of strain JMR5, including the tentative identification and annotation of extrachromosomal elements, was performed based on short-read Illumina sequence data (ERS2564723 from PRJEB25045) as described (Hornung et al., 2019; Crobach et al., 2022). The complete genome was generated based on long read sequencing on the Pacific Biosciences (PacBio) Sequel platform. To prepare high molecular weight total DNA, cells from 5 mL of overnight culture were pelleted and processed using the Qiagen Genomic-tip 100/g, according to the manufacturer's instructions. PacBio sequencing libraries were generated according to the manufacturer's multiplexed microbial library preparation protocol, part number 101–696-100, version 7, July 2020 release using the SMRTbell Express Template Prep Kit v2.0 with the following modifications: genomic DNA was sheared using Speed 34 on the Megaruptor 3 (Diagenode) and an additional size selection step of 6-50 kb fragments on the Blue Pippin (Sage Science) was included for the final SMRT bell library. The libraries were sequenced on a Sequel II platform (Pacific Biosciences) using the Sequel II Binding Kit v2.0, Sequencing Primer v4, Sequencing Kit v2.0 and a 30 h movie time.

2.3. Data analysis and visualization

Raw PacBio sequence data was assembled using Flye (v2.9) (Kolmogorov et al., 2019) and the start position was fixed using Circlator and the "fixstart" parameter (Hunt et al., 2015). Assembly quality was subsequently inspected using QUAST (Gurevich et al., 2013) and assembly completeness using BUSCO (v5.3.2, dataset clostridia_odb10 creation date 2020-03-06) (Manni et al., 2021). Prokka (v1.14.6) was used for rapid genome annotation and to obtain protein sequences, with the "–kingdom Bacteria", "–genus Clostridioides" and "–species difficile" parameters (Seemann, 2014). Multi-locus sequence typing (MLST) was performed using mlst (v2.19.0) with the PubMLST *C. difficile* database updated to October 21st 2021 (Jolley et al., 2018). Alignments of plasmid families were visualized using clinker (Gilchrist and Chooi, 2021). Amrfinderplus (v3.1.23) (Feldgarden et al., 2021) with the database version of December 21st 2021 was run to identify acquired antimicrobial resistance (AMR) genes, genes with point mutations conferring resistance to antimicrobials (specifically *gyrA*, *gyrB*, *murG*, *rpoB*, *rpoC* and *23S*) and virulence factors (including the *C. difficile* toxin genes) with the following options: "-n" "–organism Clostridioides_difficile","—plus". The MobileElementFinder (Johansson et al., 2021), ISFinder (https://www-is.biotoul.fr/search.php), TnCentral (https://tncentral.proteininformationresource.org/index.html) and PHASTER (Arndt et al., 2016) webservers were used to detect potential mobile elements and (pro)phages with default settings. To calculate

mean read depth, Illumina reads were mapped onto the complete genome (chromosome and plasmids) using minimap2 (v2.24-r1122) (Li, 2018). The obtained alignment file was indexed and sorted using samtools (v1.15.1) and samtools depth was used to compute the read depth at each position of the chromosome, while samtools coverage was used to obtain the mean depth per contig (chromosome and plasmids) (Li et al., 2009).

All figures were prepared using software from Adobe Photoshop and Illustrator 2021 (Adobe, Inc.), using exports from the tools indicated above.

2.4. Data and code availability

Raw sequence data generated for this study is available at the European Nucleotide Archive under BioProject PRJEB53950. All bioinformatic tools used for the analyses are freely available through the references provided. Plasmid sequences have also been deposited independently as ON887052 (pJMR5–1), ON887053 (pJMR5–4) and ON887054 (pJMR5-W) in GenBank. The complete genome sequence of JMR5 is GCA_944989955.1 (assembly)/ERS12289077 (sample). Previously generated whole genome sequences (Crobach et al., 2022) are available under BioProject number PRJEB25045. Sequences for pCD-ECE1 (LR594544.1), pCD-ECE4 (LR594545.1), pCD630 (AM180356.2) and pCD-WTSI1 (MG019959.1) were retrieved from GenBank.

2.5. Confirmation of extrachromosomal nature of the plasmids

In order to confirm the extrachromosomal nature of the plasmids, a PlasmidSafe DNase (PSD; Epicentre) experiment was performed as described previously (Boekhoud et al., 2020). In short, total genomic DNA was isolated and incubated in the presence or absence of PSD for 24 h. Chromosomal DNA is fragmented and susceptible for degradation by PSD in this procedure, whereas small circular double stranded DNA (plasmids) is not. After incubation, the remaining DNA was purified and amplified with primers specific for loci on the chromosome (oWKS-1070/oWKS-1071), pJMR5–1 (oAR-1/oAR-2), pJMR5–4 (oAR-3/oAR-4) and pJMR5-W (oAR-5/oAR-6) using MyTaq DNA polymerase (Meridan) according to the instructions of the manufacturer. The sequences of all oligonucleotides are listed in Table 2. The obtained DNA fragments were separated on a 1% agarose 0.5× TAE (20 mM Tris, 10 mM acetic acid, 0.5 mM EDTA) gel, stained with ethidium bromide and imaged on an Essential V6 imaging platform (Uvitec).

2.6. Molecular biology procedures

A series of vectors was constructed harboring fragments of the pJMR5-plasmids, to determine regions that are functional as a replicon in *C. difficile*. All vectors were constructed with restriction/ligation cloning using a linearized pAP24-based vector (Oliveira Paiva et al., 2016) as the backbone and a DNA fragment of interest as insert. Plasmids were isolated from 1 mL overnight culture using NucleoSpin Plasmid Easypure columns (Macherey-Nagel) from the Plasmid Easypure Kit (Nucleospin).

Putative replicon fragments were obtained through amplification PCR using high fidelity enzyme Q5 DNA polymerase (NEB) and primers including a *KpnI* or *NcoI* restriction site (Table 2). After digestion with *KpnI*/*NcoI*, the amplicons were ligated into similarly digested pAP24-backbone (Oliveira Paiva et al., 2016), as described previously (Boekhoud et al., 2020), and transformed to *E.coli* DH5α with selection on chloramphenicol-containing LB agar plates. All constructs were verified

Table 2
Oligonucleotides used in this study. Relevant restriction sites are underlined.

Name	Sequence 5′ > 3′	Description	Reference
oAR-1	TTGATTTATTTTTATAGTGGAACTAATGGC	pJMR5–1 Forward	This study
oAR-2	ACACCATACCAAGTATAAACAGC	pJMR5–1 Reverse	This study
oAR-3	AGGTATGGAGCAATCAGAAAAAG	pJMR5–4 Forward	This study
oAR-4	GTTTTTTATAATCTTCTGGTTGCATGTG	pJMR5–4 Reverse	This study
oAR-5	GGAACATGATTTATATAGCCTAATAAT	pJMR5-W Forward	This study
oAR-6	CTGTCACAGGGTTTGGAAG	pJMR5-W Reverse	This study
oAR-12	GTGGTACCTCAACATCATTAAAAGTAACTATCA	Cloning of pJMR5–1 replicon Forward	This study
oAR-13	CTCCCATGGAATTCTTAAATAGTTTGACATTTAG	Cloning of pJMR5–1 replicon Reverse	This study
oAR-14	GTGGTACCAAAAGCACCTCCTTATAAAC	Cloning of pJMR5–1 replicon Forward	This study
oAR-15	CTCCCCATGGAGGAAGTATTTATTTGAACTTTTAG	Cloning of pJMR5–1 replicon Reverse	This study
oAR-16	GTGGTACCAGCTACTTTCAACCTTTCATG	Cloning of pJMR5-W replicon Forward	This study
oAR-17	CTCCCATGGTATTAAAACCGTCAATTATACTTTTATTAATG	Cloning of pJMR5-W replicon Reverse	This study
oAR-18	GTGGTACCAAAGTGATTTTTTATATATTATTATGAATA	Cloning of pJMR5–4 replicon Forward	This study
oAR-19	CTCCCATGGCTAATTTTTATTAACTAATCTACTTACT	Cloning of pJMR5–4 replicon Reverse	This study
oAR-20	GTGGTACCTATGTGAAGAAGAATGATTTATATG	Cloning of pJMR5–4 replicon Forward	This study
oAR-21	AAAACGGCTTAATTTCAATAC	Sequencing replicons	This study
oAR-22	CCATACTCACTTTTGCCC	Sequencing replicons	This study
oAR-23	ACATGCTACAGAAGGTAAGAACGT	Sequencing replicons	This study
oAR-24	GGTATCTTATCATATGCACC	Sequencing replicons	This study
oAR-25	CTTTAGGTAGTCAAAAAGC	Sequencing replicons	This study
oAR-26	CCATTGAATTTTATGAATGAATATG	Sequencing replicons	This study
oAR-27	AGGTCTATTCGTATCAGC	Sequencing replicons	This study
oAR-28	GCCTAGTATATCATCGCAG	Sequencing replicons	This study
oAR-29	GTATAAATAGTCACATAACTCTATAG	Sequencing replicons	This study
oAR-31	CTCCCATGGTGTATGATTTTCTTTGCTGTTTTTAC	Cloning of pJMR5-W replicon Reverse	This study
oAR-36	ATGCTATGTTTTGATGAGTATATGCT	Sequencing replicons	This study
oAR-37	CTGTACGTTTGTTAATTTAGTTTAAGTGA	Sequencing replicons	This study
oWKS-1070	GTCTTGGATGGTTGATGAGTAC	Targeting chromosome (*gluD* Forward)	(Smits et al., 2018)
oWKS-1071	TTCCTAATTTAGCAGCAGCTTC	Targeting chromosome (*gluD* Reverse)	(Smits et al., 2018)
oWKS-1387	CAGATGAGGGCAAGCGGATG	Verification of transconjugants (*traJ* Forward)	(Boekhoud et al., 2020)
oWKS-1388	CGTCGGTGAGCCAGAGTTTC	Verification of transconjugants (*traJ* Reverse)	(Boekhoud et al., 2020)
oWKS-1633	AAAGTAGTTACGGGCGACAC	Targeting pCD630	(Smits et al., 2018)
oWKS-1634	TCACAGAAGGCTGCAAACTC	Targeting pCD630	(Smits et al., 2018)

by Sanger sequencing using primers listed in Table 2.

For conjugation, *E.coli* CA434 competent cells (Purdy et al., 2002) were transformed using purified plasmid DNA and transformants were selected on LB agar supplemented with chloramphenicol and kanamycin. Conjugative transfer of the plasmids from CA434 to *C. difficile* 630Δ*erm* (van Eijk et al., 2015) was performed according to standard procedures (Purdy et al., 2002). The transconjugants, selected on thiamphenicol containing media, were screened with PCR using MyTaq DNA polymerase (Meridan) directly on colony material or on purified DNA. DNA extractions were performed using the DNeasy Blood and Tissue (Qiagen) kit after enzymatic cell lysis as prescribed by the manufacturer. To confirm identity of the transconjugants, the presence of *gluD* (on the chromosome) and *traJ* (on the plasmid backbone) was verified in a PCR using primers oWKS-1070/oWKS-1071 and oWKS-1387/oWKS-1388, respectively (Table 2). The presence of the pCD630 plasmid in the DNA samples of the transconjugants was confirmed by performing a PCR using primers oWKS-1633 and oWKS-1634 (Table 2).

For determination of conjugation efficiency, conjugations were performed as follows. For each plasmid, conjugations were performed in biological triplicate. Cells from the equivalent of 1 mL of culture with OD_{600nm} of 1 of CA434 donors containing the relevant plasmid were resuspended in 200 uL of an overnight culture of *C. difficile* 630Δ*erm* (van Eijk et al., 2015), spotted onto a BHIY agar plate and incubated for 22 h. Growth from individual conjugation plates was harvested into 4 mL prereduced BHIY medium and a serial dilution was prepared in the same medium. To enumerate transconjugants, undiluted sample was plated onto prereduced BHIY agar with 50 μg/mL colistin (to eliminate the CA434 donor cells) and 15 μg/mL thiamphenicol (to select for the plasmids) using a Whitley WASP Touch spiral plater (Don Whitley Scientific). To enumerate the total number of *C. difficile* recipient cells, a 10^{-5} dilution of the suspension was similarly plated onto prereduced BHIY agar supplemented with 50 μg/mL colistin only. After 24 h incubation, colonies were counted and converted to CFU/mL using a Scan 500 automated colony counter (Interscience). Conjugation efficiency was calculated as [CFU/mL transconjugants]/[CFU/mL of recipient cells]. With a 100 μL logarithmic spiral deposition, the limit of detection of the WASP Touch is 200 CFU/mL (according to the manufacturer's information). Based on enumeration of recipient *C. difficile* cells, this places the limit of detection in this assay at a conjugation efficiency of $\sim 1 \times 10^{-10}$. Zero-values were set to our limit of detection and data were plotted using the geom_boxplot function (ggplot v3.3.6) in R 4.2.0 (https://www.R-project.org/).

3. Results and Discussion

3.1. Characterization of the plasmid-containing isolates

The four strains described in this study (JMR1, JMR2, JMR5 and JMR7) were obtained from a symptomatic patient suffering from recurrent *Clostridioides difficile* infection. Molecular diagnostics and analysis of previously generated whole genome sequencing data confirmed that all isolates are of the same PCR ribotype (RT081), have the same toxin profile and are indistinguishable in a core genome MLST analysis (Supplemental Material).

Carriage of extrachromosomal elements was predicted according to established methods (Hornung et al., 2019). The predictions indicate possible extrachromosomal elements belonging to the pCD-ECE1, pCD-ECE4 and pCD-WTSI1 families (Hornung et al., 2019). We extracted the contigs corresponding to the predicted extrachromosomal elements, and circularized them after removal of the terminal repeats, yielding sequences of 6.5, 15.4 and 21.9 kb size, respectively. As the sampling dates of the isolates span a period of several months, these data suggest that patients can be persistently infected with a strain that carries multiple plasmids.

3.2. Confirmation of the extrachromosomal nature of pJMR5–1, pJMR5–2 and pJMR5–3

To confirm the presence and the circular dsDNA nature of the elements *in vivo*, we performed a PlasmidSafe DNase (PSD) analysis using primers specifically directed at regions of each putative plasmid (Smits et al., 2018). Though the method has its limitations (Smits et al., 2022), it has been used for this purpose with *C. difficile* isolates before (Boekhoud et al., 2020; Cizek et al., 2022). The PSD analysis showed that a product of the expected size was obtained in PCRs targeting each of the putative plasmids, even for PSD-treated samples. In contrast, a PCR product for the chromosomal locus *gluD* was only obtained in the samples that were not treated with PSD (Fig. 1). We note a decrease in the strength of the signal on gel for the pCD-WTSI family plasmid upon treatment with PSD; as this is the largest of the predicted plasmid, we attribute this to partial fragmentation of the dsDNA during the DNA isolation.

These data indicate that all JMR strains contain circular dsDNA that is extrachromosomal, consistent with the presence of a plasmid.

3.3. Complete genome sequence of C. difficile *JMR5*

Next, we determined the complete genome sequence of JMR5, as a representative of the group of JMR strains, using single molecule real time sequencing. Assembly of the reads of the Pacific Bioscience Sequel platform yielded a single circular chromosome of 4.3 Mb and 3 smaller contigs (Supplemental Fig. 1). The size and sequence of the latter matched the predicted circular elements discussed above, and are hereafter referred to as pJMR5–1 (for plasmid from **JMR5** from the pCD-ECE1 family; ON887052), pJMR5–4 (for plasmid from **JMR5** from the pCD-ECE4 family; ON887053) and pJMR5-W (for plasmid from **JMR5** from the pCD-WTSI1 family; ON887054). Initially, we recovered only pJMR-4 and pJMR5-W in the *de novo* assembly, possibly as a result of size selection during the library preparation (see Materials and Methods). However, manual inspection of the data revealed a significant number of reads matching pJMR5–1 and these reads fully matched the predicted sequence; indeed, altering the default settings of Flye (Kolmogorov et al., 2019) allowed automatic recovery of the pJMR5–1 plasmid, though in this case the plasmid contained a duplication (a well-known artefact of long-read sequencing of small plasmids) (Hunt et al., 2015). No other extrachromosomal elements were assembled with <0.05% of the long reads remaining unassembled. This shows that no other extrachromosomal elements are present that might have been missed in our computational approach (Smits et al., 2022; Hornung et al., 2019).

The genome of JMR5 is 4.321.867 bp and has an average [G + C]-content of 29.0%, in line with other *C. difficile* genomes. An automated annotation identifies 3937 ORFs, 35 rRNA genes,90 tRNA genes and a single tmRNA. Plasmids pJMR5–1, pJMR5–4 and pJMR5-W plasmids had a [G + C]-content of 25.2, 25.5 and 31.1% and encode 11, 18 and 26 ORFs, respectively (Supplemental Table S1).

Several AMR genes were identified by AMRfinderplus (Feldgarden et al., 2021) on the JMR5 chromosome, namely *bla-CDD1*, *erm*(B), the *vanG*Cd operon and a T82I point mutation in *gyrA*, associated with fluoroquinolone resistance. One AMR gene, *tet*(M), was present on pJMR5-W. The *erm*(B) gene is predicted by TnCentral (https://tncentral.proteininformationresource.org/index.html) to be on a Tn*551*/Tn*917*-like element (similar to Y13600.1; e-value 0.0). ISFinder (https://www-is.biotoul.fr/search.php) identifies three IS elements with an e-value <0.01, but homology is limited to regions <40 bp. No mobile elements were identified by MobileElementFinder (Johansson et al., 2021). PHASTER (Arndt et al., 2016), finally, predicts intact phages (score > 90) similar to CDMH1 (NC_024144), phiMMP03 (NC_047770) and phiMMP01 (NC_028883) as well as three incomplete phages.

We used PubMLST (Jolley et al., 2018) to predict the sequence type of JMR5. The isolate was identified as belonging to ST9, consistent with

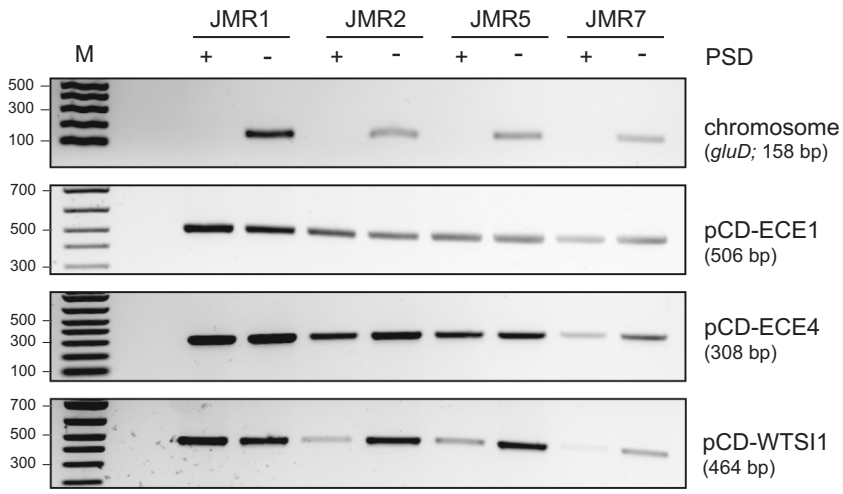

Fig. 1. JMR strains contain three plasmids. Total genomic DNA was incubated in the absence (−) or presence (+) of PlasmidSafe DNase (PSD) and subsequently amplified with primers specific for the indicated DNA (*gluD*: oWKS1070/1071, pCD-ECE1 family: oAR1/2, pCD-ECE4 family: oAR3/4, pCD-WTSI1 family: oAR4/5; see Table 2 and Materials and Methods). The expected size in base pairs is indicated. M: 100-bp marker.

previous studies that place the RT081 reference strain from the Leeds-Leiden collection in the same sequence type (Knetsch et al., 2012; Baktash et al., 2022).

3.4. Comparison of the identified plasmids with reference plasmids

The tentative assignment of the three plasmids to the pCD-ECE1, pCD-ECE4 and pCD-WTSI1 family of plasmids is based on regions of similarity with the reference sequences for these plasmids as described (Hornung et al., 2019). To gain more insight in the relatedness of the plasmids, we generated and visualized nucleotide alignments using clinker (Gilchrist and Chooi, 2021). From these analyses, multiple observations were made.

First, we note that the ORF7-ORF8 region of pCD-ECE1 appears not to be conserved in pJMR5–1 (Fig. 2A). This was unexpected, as ORF8 of pCD-ECE1 was hypothesized to encode a replication-associated protein based on limited homology to viral REP proteins (Hornung et al., 2019). If this region of the plasmid is involved in replication, the corresponding region in pJMR5–1 should also encode a replication protein. Indeed, analysis of the predicted amino acid sequence of the pJMR5–1 protein using the PHYRE2 Protein Fold Recognition Server (Kelley and Sternberg, 2009) indicates that it likely is a rolling circle replication initiator protein (PDB 4CIJ; confidence 98.8%; identity; 13%). As most pCD-ECE1 family plasmids that are predicted to be circular match the pCD-ECE1 reference sequence (LR594544.1) (Hornung et al., 2019), the mechanism of replication for pJMR5–1 may be different from those.

Second, the pJMR5–4 plasmid appears to contain a 11-gene insertion in comparison to the pCD-ECE4 reference sequence (Fig. 2B), consistent

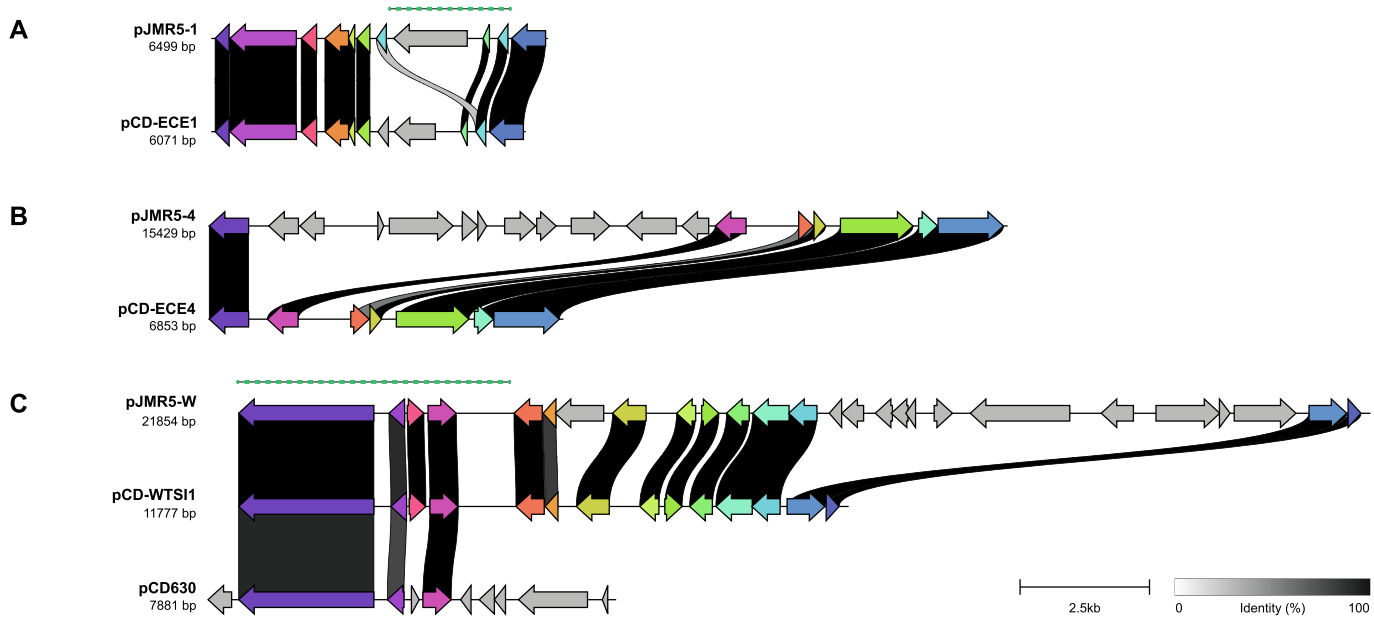

Fig. 2. Comparison of pJMR5 plasmids with reference plasmids. Within panels, colored arrows indicate similar genes; links are drawn between similar genes on neighboring clusters and are shaded based on sequence identity (0% white, 100% black, identity threshold for visualization 0.30). Dashed green lines indicate regions capable of sustaining replication of a shuttle vector in *C. difficile*. A. Comparison of pJMR5–1 (ON887052) with pCD-ECE1 (LR594544.1). B. Comparison of pJMR5–4 (ON887053) with pCD-ECE4 (LR594545.1). C. Comparison of pJMR5-W (ON887054) with pCD630 (AM180356.2) and pCD-WTSI1 (MG019959.1). Image is based on a visualization with clinker (Gilchrist and Chooi, 2021). (For interpretation of the references to colour in this figure legend, the reader is referred to the web version of this article).

with a previously reported large size-diversity within this family (Hornung et al., 2019). Automated annotation of gene function (see Materials and methods) suggests that this region may include a methylation sensitive restriction modification system as ORF12 of pJMR5–4 encodes a putative type II endonuclease, and ORF11 encodes a DNA (cytosine-5-)-methyltransferase. We note that in a previous *in silico* analysis several pCD-ECE4 family plasmids were identified that match in size to pJMR5–4 (Hornung et al., 2019), whereas the majority matches the pCD-ECE4 reference sequence (LR594545.1). This suggests that the 11-gene insertion is conserved in a subset of plasmids from this family.

Third, pJMR5-W is substantially larger than other members of the pCD630/pCD-WTSI1 family (Fig. 2C) (Smits et al., 2018). Plasmids pCD630 and pCD-WTSI1 share a conserved region that encodes a helicase protein, believed to be important for replication, but differ in their accessory genes (Smits et al., 2018). pJMR5-W also contains the conserved region but it appears that pJMR5-W contains two insertions compared to pCD-WTSI1; i) a single hypothetical gene that is also found at this site for other pCD-WTSI family plasmids (Smits et al., 2018) and ii) an 11-gene cluster suggestive of a mobile element (*e.g.* including a gene encoding an Tn*916*-like excisionase [ORF23] and an integrase [ORF24]). Interestingly, PHYRE2 (Kelley and Sternberg, 2009) also predicts multiple regulator proteins (ORF14, ORF15, ORF19, ORF21), a putative rolling circle replication initiator protein (PDB 4CIJ, confidence 100, 28% identity), and a putative tetracycline resistance protein (ORF20)(PDB 3J25, confidence 100, 97% identity) in the island. Tn*916*-like elements are common vehicles for tetracycline resistance genes (Roberts and Mullany, 2011).

3.5. A functional replicon from pJMR5–1 and pJMR5-W

Based on the sequence analysis, we expected ORF8 of pJMR5–1 to be required for replication of the plasmid in *C. difficile*. To assess which region is sufficient for replication, we replaced the pCD6 replicon from an established *E.coli-C. difficile* shuttle vector (Oliveira Paiva et al., 2016) with different, but overlapping, regions of the pJMR5–1 plasmid. The obtained constructs were conjugated into the *C. difficile* laboratory strain 630Δ*erm* (van Eijk et al., *2015*; Hussain, *2005)*; when transconjugants were obtained this was taken as a sign of a functional replicon, whereas repeated failure to obtain transconjugants suggested that a critical determinant was missing (the limit of detection under our experimental conditions is a conjugation efficiency of $\sim 1 \times 10^{-10}$). A region encompassing ORF7-ORF10 sustained plasmid replication, as did a region encompassing ORF8-ORF10 as transconjugants were readily obtained when conjugating plasmids pJMR25 and pJMR51 (Table 3, Fig. 3). In contrast, a region encompassing only ORF8, or ORF7-ORF8 did not, as we failed to obtain transconjugants with plasmid pJMR20 and pJMR52 (Table 3, Fig. 3). We conclude that the ORF8-ORF10 region is sufficient to allow the plasmid to replicate (Fig. 2A). For pJMR25 we obtained a conjugation efficiency of $\sim 1.4 \times 10^{-6}$, which is in the same order of magnitude as observed for plasmid with a pCD6 replicon, pAP24 ($\sim 5.5 \times 10^{-6}$) (Fig. 3). Furthermore, preliminary data suggests that ORF10, encoding an Arc-type ribbon-helix-helix protein is essential for this function (data not shown).

Table 3
Results of conjugations.

Origin of putative replicon	Plasmid	Recipient strain	pCD630 in recipient (yes/no)	Transconjugants obtained (yes/no)[#]
pCD6	pAP24	630Δ*erm*	Yes	Yes
pCD-METRO	pIB80	630Δ*erm*	Yes	Yes
pJMR5–1	pJMR20	630Δ*erm*	Yes	No
	pJMR25	630Δ*erm*	Yes	Yes
	pJMR51	630Δ*erm*	Yes	Yes
	pJMR52	630Δ*erm*	Yes	No
pJMR5–4	pJMR33	630Δ*erm*	Yes	No
	pJMR46	630Δ*erm*	Yes	No
pJMR5-W	pJMR28	630Δ*erm*	Yes	No
		JIR8094	No	No
		DSMZ 28645	No	No
	pJMR57	630Δ*erm*	Yes	Yes
		JIR8094	No	Yes
		DSMZ 28645	No	Yes

[#] LOD = limit of detection (conjugation efficiency of $\sim 1 \times 10^{-10}$).

A previous analysis of the ORFs on the pCD-ECE4 reference sequence failed to predict a replicon region in plasmids from this family (Hornung et al., 2019). Screening the ORFs of pJMR5–4 using the current database of PHYRE2 indicated that ORF5 (in the 11-gene insert) likely encodes a protein of which the core domain shows homology to the archaeo-eukaryotic primase (AEP) domain of an archaeal primase protein (PDB 1V33; confidence 96.8, 32% identity) (Czernecki et al., 2021). However, a region encompassing this protein, or a region additionally encompassing ORF1-ORF5 and an area of high repeat-density, did not sustain plasmid replication in *C. difficile* as conjugation efficiency was below the limit of detection in our assay (Table 3). It is likely that one or more of the hypothetical genes in the conserved part of the pCD-ECE4 family of plasmids encodes a hitherto unidentified replication function.

The plasmid pJMR5-W contains the helicase-containing module that defines the pCD630/pCD-WTSI family of plasmids (Smits et al., 2018). We cloned two different fragments of the highly conserved region into a vector as potential replicons; pJMR57 carries the complete conserved region as putative replicon, and pJMR28 includes only ORF1, encoding the putative helicase protein. We considered that the pJMR5-W replicon might not be compatible with the replicon of pCD630 due to high similarity (Fig. 2B). Plasmid pCD630 is present in our recipient strain 630Δ*erm* (van Eijk et al., 2015) so two additional recipient strains were included; DSMZ 28645 (a 630Δ*erm* strain from the Leibniz Institute DSMZ collection) (Riedel et al., 2015) and JIR8094 (also known as 630E) (O'Connor et al., 2006) both of which do not contain the pCD630 plasmid (Smits et al., 2018). Conjugation of the three strains with pJMR28 (containing only the ORF9 fragment) repeatedly did not result in any growth on the selective plates, while conjugation with pJMR57 (containing the complete conserved region, including ORF1–4) did yield viable transconjugants carrying the vector (Table 3). Therefore, we conclude that the conserved region characterizing all pCD630/pCD-WTSI plasmids comprises a functional replicon, whereas a fragment encoding only the helicase is not sufficient for plasmid maintenance. The conjugation efficiency for pJMR57 was $\sim 3.3 \times 10^{-8}$, which is approximately an order of magnitude lower than observed for another well-characterized plasmid, pIB80 ($\sim 2.8 \times 10^{-7}$), and two orders of magnitude lower than pAP24 (Fig. 3). The fact that plasmid pJMR57 was successfully introduced into a recipient strain carrying pCD630 indicates that pCD630 and pCD-WTSI1 are compatible plasmids, at least for the duration of the experiment. This was confirmed by a PCR specifically targeting the pCD630 sequence on purified DNA from the obtained transconjugants (data not shown). Nevertheless, the relatively low conjugation efficiency might indicate that similar replicons do interfere with plasmid transfer or maintenance. Our experimental data is consistent with the *in silico* prediction that pCD-WTSI family plasmids appear compatible with most other plasmids, including others from the pCD-WTSI1 family (*i.e.* the replication function does not confer incompatibility) (Smits et al., 2022). Of note, our results also show that the putative rolling circle replication protein of pJMR5-W (ORF22) – that is not present in pCD-WTSI1 or pCD630 – is not strictly required for replication, despite its structural similarity to a plasmid replication protein. However, we have not yet established whether a region of the plasmid that incorporates this protein might also be able to sustain replication so we cannot rule out such a function at this time.

3.6. Plasmids with the pJMR5-W replicon have a high copy number

As the initial identification of the pJMR-plasmids was in part based

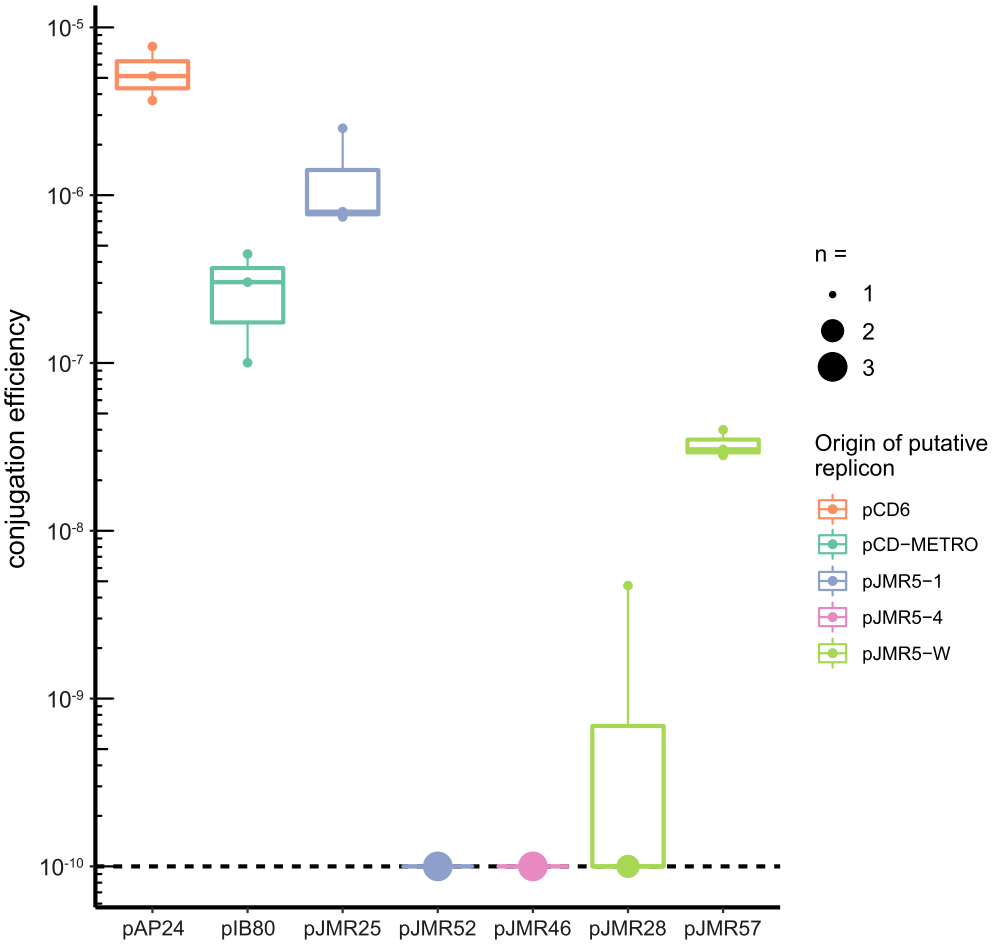

Fig. 3. Conjugation efficiency of plasmids carrying different *C. difficile* replicons. Conjugation efficiencies were determined for three independent biological replicates for the indicated plasmids. Plasmids pAP24 and pIB80 were included as well-characterized controls. The dashed line indicates the limit of detection in our assay (see Materials and Methods); when no transconjugant colonies were obtained in the assay, the value was set to 10^{-10}. Individual datapoints are shown, and boxplots represent the median (horizontal line), range between the 1st and 3rd quartile (box) and the distance to the most distant value (no >1.5-times the interquartile range). We consider the non-zero value for pJMR28 (the result of a single colony) to be an outlier.

on differences in read depth between chromosomal and extrachromosomal contigs (Hornung et al., 2019), we expected the plasmids to be multi-copy. Indeed, when mapping the short-read sequencing to the complete genome sequence of JMR5 (GCA_944989955.1) we found that chromosomal loci show a mean read depth of 265, whereas the plasmids show a mean read depth of 3039 (pJMR5–1), 3402 (pJMR5–4) and 5680 (pJMR5-W), translating to a relative copy number of 11.4, 12.8 and 21.4, respectively (Fig. 4). We observed a higher read depth of regions proximal to the origin of replication of the chromosome (Fig. 4**; inset**), as is expected from replicating cells (van Eijk et al., 2019; Slager and Veening, 2016). A chromosomal region with higher-than-expected read depth corresponds to the phiMMP01-like phage (section 3.3), suggesting that this phage may show a partially extrachromosomal lifecycle under the conditions analyzed (**arrow,** Fig. 4**, inset**).

As the replicons of pJMR5-W and pCD630 are highly related, we consider it likely that pCD630 has a similarly high copy number, which might contribute to its segregational stability in the absence of selection (Smits et al., 2018).

4. Conclusions

In this study we demonstrated carriage of three different plasmids in

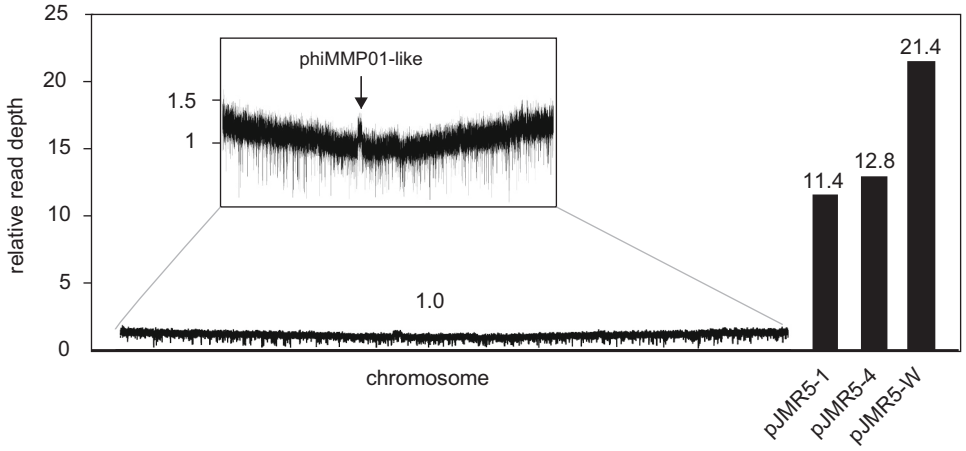

Fig. 4. Relative read depth of chromosome and plasmids of isolate JMR5. Chromosomal read depth was calculated per base pair and plotted *versus* position on the chromosome. Mean read depth for plasmids was calculated for the entire plasmid and normalized against the mean read depth of the chromosome and values are indicated above the graph and bars. Note that the width of the bars is not proportional to the chromosome. The inset shows that chromosomal read coverage is not uniform but shows a pattern consistent with bidirectional DNA replication.

a clinical isolate obtained from a symptomatic patient suffering from recurrent CDI. Importantly, epidemiological evidence suggests that the pJMR5–1, pJMR5–4 and pJMR5-W plasmids are retained during a persistent infection over a period of months. We additionally showed that regions encompassing ORF8–10 of pJMR5–1 and ORF1–4 of pJMR5-W are sufficient to sustain multiple plasmid copies per cell in *C. difficile*, with plasmids harboring the pJMR5–1 replicon resulting in conjugation frequencies similar to well-characterized shuttle vectors.

Supplementary data to this article can be found online at https://doi.org/10.1016/j.plasmid.2022.102669.

Funding

This research did not receive any specific grant from funding agencies in the public, commercial, or not-for-profit sectors.

CRediT authorship contribution statement

Anna M. Roseboom: Investigation, Formal analysis, Writing – review & editing. **Quinten R. Ducarmon:** Formal analysis, Writing – original draft, Visualization, Writing – review & editing. **Bastian V.H. Hornung:** Conceptualization, Methodology, Formal analysis, Writing – review & editing. **Céline Harmanus:** Investigation, Writing – review & editing. **Monique J.T. Crobach:** Formal analysis, Writing – review & editing. **Ed J. Kuijper:** Supervision, Writing – review & editing. **Rolf H.A.M. Vossen:** Investigation, Formal analysis, Writing – review & editing. **Susan L. Kloet:** Project administration, Supervision, Resources, Writing – review & editing. **Wiep Klaas Smits:** Conceptualization, Investigation, Formal analysis, Visualization, Project administration, Resources, Writing – original draft, Writing – review & editing.

Declaration of Competing Interest

None.

Data availability

All resources are freely available and data has been deposited in appropriate public repositories.

Acknowledgements

The authors would like to acknowledge B. Nibbering for isolating the total genomic DNA for PacBio sequencing, S. Nooij for assistance with PacBio-data analysis and I. Sidorov for the local implementation of clinker at the LUMC. The authors are indebted to R. Fagan for making the suggestion to use colistin as a counterselection in the conjugation efficiency experiments.

References

Adams, V., Li, J., Wisniewski, J.A., Uzal, F.A., Moore, R.J., McClane, B.A., et al., 2014. Virulence plasmids of spore-forming Bacteria. Microbiol. Spectr. 2.

Arndt, D., Grant, J.R., Marcu, A., Sajed, T., Pon, A., Liang, Y., et al., 2016. PHASTER: a better, faster version of the PHAST phage search tool. Nucleic Acids Res. 44, W16–W21.

Baktash, A., Corver, J., Harmanus, C., Smits, W.K., Fawley, W., Wilcox, M.H., et al., 2022. Comparison of whole-genome sequence-based methods and PCR Ribotyping for subtyping of *Clostridioides difficile*. J. Clin. Microbiol. 60, e0173721.

Boekhoud, I.M., Hornung, B.V.H., Sevilla, E., Harmanus, C., Bos-Sanders, I., Terveer, E. M., et al., 2020. Plasmid-mediated metronidazole resistance in *Clostridioides difficile*. Nat. Commun. 11, 598.

Cizek, A., Masarikova, M., Mares, J., Brajerova, M., Krutova, M., 2022. Detection of plasmid-mediated resistance to metronidazole in *Clostridioides difficile* from river water. Microbiol. Spectr. 10 (4), e0080622 https://doi.org/10.1128/spectrum.00806-22.

Crobach, M.J.T., Hornung, B.V.H., Verduin, C., Vos, M.C., Hopman, J., Kumar, N., et al., 2022. *Clostridioides difficile* Colonization at Admission to the Hospital and Onwards Transmission: A Multi-Centre Case-Control Study. Submitted.

Czernecki, D., Legrand, P., Tekpinar, M., Rosario, S., Kaminski, P.A., Delarue, M., 2021. How cyanophage S-2L rejects adenine and incorporates 2-aminoadenine to saturate hydrogen bonding in its DNA. Nat. Commun. 12, 2420.

ECDC, 2018. Laboratory Procedures for Diagnosis and Typing of Human *Clostridium difficile* Infection. Stockholm. https://www.ecdc.europa.eu/sites/default/files/documents/SOPs-Clostridium-difficile-diagnosis-and-typing.pdf.

Fawley, W.N., Knetsch, C.W., MacCannell, D.R., Harmanus, C., Du, T., Mulvey, M.R., et al., 2015. Development and validation of an internationally-standardized, high-resolution capillary gel-based electrophoresis PCR-ribotyping protocol for *Clostridium difficile*. PLoS One 10, e0118150.

Feldgarden, M., Brover, V., Gonzalez-Escalona, N., Frye, J.G., Haendiges, J., Haft, D.H., et al., 2021. AMRFinderPlus and the reference gene catalog facilitate examination of the genomic links among antimicrobial resistance, stress response, and virulence. Sci. Rep. 11, 12728.

Gilchrist, C.L.M., Chooi, Y.H., 2021. Clinker & clustermap.Js: automatic generation of gene cluster comparison figures. Bioinformatics 37 (16), 2473–2475. https://doi.org/10.1093/bioinformatics/btab007.

Gurevich, A., Saveliev, V., Vyahhi, N., Tesler, G., 2013. QUAST: quality assessment tool for genome assemblies. Bioinformatics 29, 1072–1075.

Hornung, B.V.H., Kuijper, E.J., Smits, W.K., 2019. An *in silico* survey of *Clostridioides difficile* extrachromosomal elements. Microb. Genom. 5, e000926.

Hunt, M., Silva, N.D., Otto, T.D., Parkhill, J., Keane, J.A., Harris, S.R., 2015. Circlator: automated circularization of genome assemblies using long sequencing reads. Genome Biol. 16, 294.

Hussain, H.A., 2005. Generation of an erythromycin-sensitive derivative of *Clostridium difficile* strain 630 (630 erm) and demonstration that the conjugative transposon Tn*916*E enters the genome of this strain at multiple sites. J. Med. Microbiol. 54, 137–141.

Johansson, M.H.K., Bortolaia, V., Tansirichaiya, S., Aarestrup, F.M., Roberts, A.P., Petersen, T.N., 2021. Detection of mobile genetic elements associated with antibiotic resistance in *salmonella enterica* using a newly developed web tool: MobileElementFinder. J. Antimicrob. Chemother. 76, 101–109.

Jolley, K.A., Bray, J.E., Maiden, M.C.J., 2018. Open-access bacterial population genomics: BIGSdb software, the PubMLST.org website and their applications. Wellcome Open Res. 3, 124.

Kelley, L.A., Sternberg, M.J., 2009. Protein structure prediction on the web: a case study using the Phyre server. Nat. Protoc. 4, 363–371.

Knetsch, C.W., Terveer, E.M., Lauber, C., Gorbalenya, A.E., Harmanus, C., Kuijper, E.J., et al., 2012. Comparative analysis of an expanded *Clostridium difficile* reference strain collection reveals genetic diversity and evolution through six lineages. Infect. Genet. Evol. 12, 1577–1585.

Kolmogorov, M., Yuan, J., Lin, Y., Pevzner, P.A., 2019. Assembly of long, error-prone reads using repeat graphs. Nat. Biotechnol. 37, 540–546.

Li, H., 2018. Minimap2: pairwise alignment for nucleotide sequences. Bioinformatics 34, 3094–3100.

Li, H., Handsaker, B., Wysoker, A., Fennell, T., Ruan, J., Homer, N., et al., 2009. The sequence alignment/map format and SAMtools. Bioinformatics 25, 2078–2079.

Manni, M., Berkeley, M.R., Seppey, M., Zdobnov, E.M., 2021. BUSCO: assessing genomic data quality and beyond. Curr. Protoc. 1, e323.

O'Connor, J.R., Lyras, D., Farrow, K.A., Adams, V., Powell, D.R., Hinds, J., et al., 2006. Construction and analysis of chromosomal *Clostridium difficile* mutants. Mol. Microbiol. 61, 1335–1351.

Oliveira Paiva, A.M., Friggen, A.H., Hossein-Javaheri, S., Smits, W.K., 2016. The signal sequence of the abundant extracellular metalloprotease PPEP-1 can be used to secrete synthetic reporter proteins in *Clostridium difficile*. ACS Synth. Biol. 5, 1376–1382.

Pu, M., Cho, J.M., Cunningham, S.A., Behera, G.K., Becker, S., Amjad, T., et al., 2021. Plasmid acquisition alters vancomycin susceptibility in *Clostridioides difficile*. Gastroenterology 160, 941–5 e8.

Purdy, D., O'Keeffe, T.A., Elmore, M., Herbert, M., McLeod, A., Bokori-Brown, M., et al., 2002. Conjugative transfer of clostridial shuttle vectors from *Escherichia coli* to *Clostridium difficile* through circumvention of the restriction barrier. Mol. Microbiol. 46, 439–452.

Ramirez-Vargas, G., Rodriguez, C., 2020. Putative conjugative plasmids with *tcdB* and *cdtAB* genes in *Clostridioides difficile*. Emerg. Infect. Dis. 26, 2287–2290.

Ransom, E.M., Ellermeier, C.D., Weiss, D.S., 2015. Use of mCherry red fluorescent protein for studies of protein localization and gene expression in *Clostridium difficile*. Appl. Environ. Microbiol. 81, 1652–1660.

Riedel, T., Bunk, B., Thurmer, A., Sproer, C., Brzuszkiewicz, E., Abt, B., et al., 2015. Genome resequencing of the virulent and multidrug-resistant reference strain *Clostridium difficile* 630. Genome Announc. 3.

Roberts, A.P., Mullany, P., 2011. Tn*916*-like genetic elements: a diverse group of modular mobile elements conferring antibiotic resistance. FEMS Microbiol. Rev. 35, 856–871.

Schwarz, S., Shen, J., Wendlandt, S., Fessler, A.T., Wang, Y., Kadlec, K., et al., 2014. Plasmid-mediated antimicrobial resistance in staphylococci and other Firmicutes. Microbiol. Spectr. 2.

Seemann, T., 2014. Prokka: rapid prokaryotic genome annotation. Bioinformatics 30, 2068–2069.

Slager, J., Veening, J.W., 2016. Hard-wired control of bacterial processes by chromosomal gene location. Trends Microbiol. 24, 788–800.

Smits, W.K., Lyras, D., Lacy, D.B., Wilcox, M.H., Kuijper, E.J., 2016. *Clostridium difficile* infection. Nat. Rev. Dis. Primer. 2, 16020.

Smits, W.K., Weese, J.S., Roberts, A.P., Harmanus, C., Hornung, B., 2018. A helicase-containing module defines a family of pCD630-like plasmids in *Clostridium difficile*. Anaerobe 49, 78–84.

Smits, W.K., Roseboom, A.M., Corver, J., 2022. Plasmids of *Clostridioides difficile*. Curr. Opin. Microbiol. 65, 87–94.
van Eijk, E., Anvar, S.Y., Browne, H.P., Leung, W.Y., Frank, J., Schmitz, A.M., et al., 2015. Complete genome sequence of the *Clostridium difficile* laboratory strain 630Deltaerm reveals differences from strain 630, including translocation of the mobile element CTn*5*. BMC Genomics 16, 31.
van Eijk, E., Boekhoud, I.M., Kuijper, E.J., Bos-Sanders, I., Wright, G., Smits, W.K., 2019. Genome location dictates the transcriptional response to PolC inhibition in *Clostridium difficile*. Antimicrob. Agents Chemother. 63.
Vedantam, G., Clark, A., Chu, M., McQuade, R., Mallozzi, M., Viswanathan, V.K., 2012. *Clostridium difficile* infection: toxins and non-toxin virulence factors, and their contributions to disease establishment and host response. Gut Microbes 3, 121–134.